Spin-orbit excitons and electronic configuration of the 5d⁴ band insulator Sr₃Ir₂O₇F₂

Zach Porter,¹ Paul M. Sarte,^{1,2} Thorben Petersen,³ Satoshi Nishimoto,³ Ulrich K. Rößler,³ Mary H. Upton,⁴ Liviu Hozoi,³ and Stephen D. Wilson^{1,2}

Materials Department, University of California, Santa Barbara, California 93106-5050, USA
² California NanoSystems Institute, University of California, Santa Barbara, California 93106-6105, USA
³ Institute for Theoretical Solid State Physics, Leibniz-IFW Dresden, Helmholtzstraße 20, D-01069 Dresden, Germany
⁴ Advanced Photon Source, Argonne National Laboratory, Argonne, Illinois 60439, USA
(Dated: November 14, 2023)

We report on the energy- and momentum-dependence of low-energy excitations in the Ir^{5+} band insulator $Sr_3Ir_2O_7F_2$, as revealed by resonant inelastic x-ray scattering (RIXS). This material is composed of corner-sharing planes of IrO_6 arranged in bilayers as in the precursor material $Sr_3Ir_2O_7$. Quantum chemistry simulations suggest that the strong departure from octahedral symmetry results in large single-ion anisotropy and causes an approximately S=1 (L=1, J=0) ground state. Weakly dispersive modes ≤ 0.6 eV are well-described by spin-orbit excitons. The couplings between excitons are too weak to yield gapless excitations yet they are relevant to the thermodynamics of this d^4 system. The results of this study's spin-orbit exciton theoretical model are extended to other d^4 and d^5 systems.

I. INTRODUCTION

Recently, a great experimental effort has begun to explore the magnetism of previously unconsidered $4d^4$ and $5d^4$ systems with octahedral ligand coordination. Such systems host J=0 singlet ground states, which naïvely yield band insulators without static magnetic order. But lately researchers have been searching for a material example, motivated by a transformative theoretical framework by Khaliullin, [1] which proposed that with strong spin-orbit coupling (SOC) the Van Vleck-type bosonic J=0 to J=1 excitations can condense into so-called 'excitonic' magnetism. One exciting aspect of this proposal is the proximity to a quantum critical point with high energy scales.[2] And, for some material realizations, the condensed phase itself could support novel spin-liquid ground states. Even though the materials studied so far (including the one in this study) may lack static magnetism arising from spin-orbit excitons, the thermodynamic signatures and phase phenomena of this fascinating class of materials is rich and little explored.

For the octahedrally coordinated $4d^4$ and $5d^4$ materials there are uncertainties regarding the electronic configuration, which draws into question the applicability of theoretical predictions for spin-orbit excitons and the broader magnetic phase behavior. Generally, the ground states for these systems are considered in two limits:

- (i) when SOC is much weaker than correlations, the triply degenerate t_{2g} manifold hosts a S=1 (L=1, J=0) state;
- (ii) when SOC is much stronger than correlations, the $J_{\rm eff}$ =3/2 doublet is filled yielding a $J_{\rm eff}$ =0 state.

However, the comparable energy scales of SOC (parameterized as $\alpha' \lambda$ with $\alpha' = \frac{1}{2})[3]$ and correlations (considered via the Hund's coupling J_H or the unscreened on-site Coulomb interaction U) for $4d^4$ and $5d^4$ compounds are

difficult to reconcile with either of these limits. As additional sources of complication, ligand hybridization has been predicted to modify filling;[4] itinerancy can mix groundstate wavefunctions; [5] and distortions from the octahedral crystal field are known to split states. The effects of these deviations from the ideal case are especially noticeable in excited states. Thus, without relying on sophisticated quantum chemistry calculations, it is difficult to compare experimentally observed electronic excitations to theoretical predictions of d^4 magnetism.

Here we study a compound derived from the wellstudied Ir⁴⁺ material Sr₃Ir₂O₇. Via a topochemical transformation on single-crystalline samples, fluorine layers are intercalated between the bilayers of corner-sharing IrO₆ octahedra. [6] The fluorine ions act to hole-dope each Ir ion to the 5+ valence. The magnetic ground state is near-fully quenched, amounting to about 1% of Ir sites with spin-1/2 moments. Crucially, this hole-doping is accomplished without diluting the lattice; each Ir ion is still nearest-neighbor coupled to 1 interlayer and 4 intralayer Ir ions (via superexchange across one O ion). And, owing to the constituent elements, we expect negligible Ir antisite defects. The resultant compound has a strong deviation from an octahedral crystal field, in contrast to Sr₃Ir₂O₇.[6] Its spin-orbit singlet S=1 (L=1, J=0) ground state, with its first excited states resembling the $S_z=\pm 1$ states, makes the present system relevant to other tetragonally distorted compounds such as Ca₂RuO₄. [7]

We use resonant inelastic x-ray spectroscopy (RIXS) to measure low-energy excitations in $Sr_3Ir_2O_7F_2$. Through this study, we measure weakly coupled spin-orbit excitons and d-d excitations to establish the energy scales of SOC, correlations, and crystal field splitting in this novel material. This work allows for quantitative comparisons to other d^4 materials like Ca_2RuO_4 and $(Sr,Ba)_2YIrO_6$.

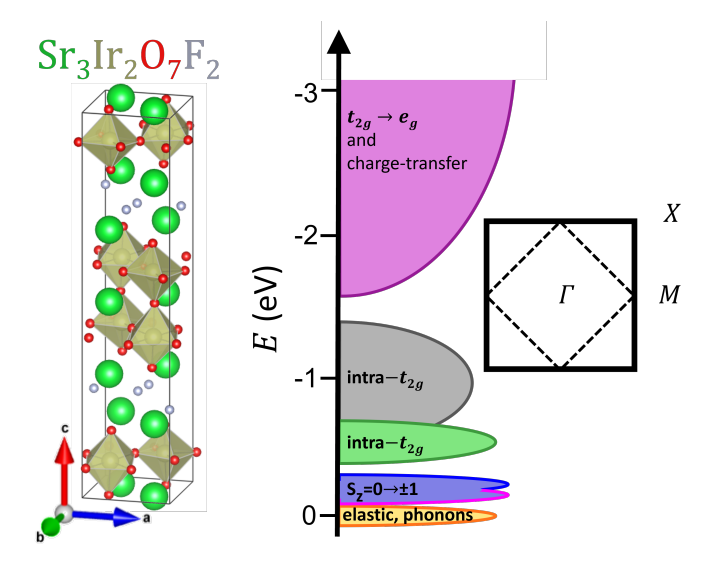


FIG. 1. Orthorhombic Bbcb unit cell (left) and quasi-2d Brillouin zone (right) for $Sr_3Ir_2O_7F_2$. Ir-O bond lengths are appreciably compressed along c near the fluorine planes. Cartoon of the excitations observed in RIXS measurements (center). Details are in the text.

II. METHODS

Sample preparation via topochemical conversion has been described elsewhere.[6] The exact synthetic conditions and further characterization are described in the Supplementary Information §S1.

Resonant inelastic x-ray scattering (RIXS) measurements were performed at Beamline 27-ID-B of the Advanced Photon Source at Argonne National Laboratory. The incident photons were tuned to the Ir L_3 absorption edge ($E=11.215~{\rm keV}$) and final energies were selected with the Si (8,4,4) reflection of a spherical analyzer crystal array in a horizontal scattering geometry. Excitations were mapped primarily in the quasi-2d l=30.5 Brillouin zone (BZ). This l value was chosen because it is far from Bragg peaks and near 2θ =90° where Thomson scattering (i.e. elastic charge scattering) is minimized.

Momentum space positions are indexed using an orthorhombic Bbcb unit cell with lattice parameters a=5.45 Å, b=5.51 Å, and c=24.21 Å; see Figure 1. This simplification from the proper C2/c cell was chosen for comparison to other quasi-2d samples. Due to twin structural domains, we do not distinguish between a and b axes. RIXS measurements were sample-resolution-limited in momentum, approximately 0.2 Å $^{-1}$, due to the high mosaicity of samples after the topochemical conversion. Detected energy resolution was ≈ 35 meV. Unless otherwise stated, measurements were performed at 8(2) K.

To determine the ground state and excited states measured via RIXS, we performed *ab initio* quantum chemistry calculations on an isolated $({\rm IrO_6})^{7-}$ monomer as well as a cluster $({\rm Ir_2O_{11}})^{12-}$... [Thorben please fill this

in

To supplement the quantum chemistry calculations, we modeled our experimental dispersion relations with a spin-orbit exciton model that relies on a single-ion Hamiltonian $\hat{\mathcal{H}}_{S.I.}$. This model for $Sr_3Ir_2O_7F_2$ employs the same formalism that was established [8] for the d^4 multiorbital Mott insulator Ca₂RuO₄. This Hamiltonian is parameterized by: $\alpha' \lambda$, H_{MF} , and δ , corresponding to the individual contributions from spin-orbit coupling, an internal mean molecular field, and a uniaxial (either tetragonal or trigonal) distortion of the local octahedral coordination environment, respectively. The resulting eigenstates of $\mathcal{H}_{S,I}$ are then coupled by the Fourier transform of the exchange interaction $J(\mathbf{Q})$, where both an isotropic nearest neighbor J_1 and next nearest neighbor exchange J_2 are considered. Refer to Supplementary Information §S3 for more details.

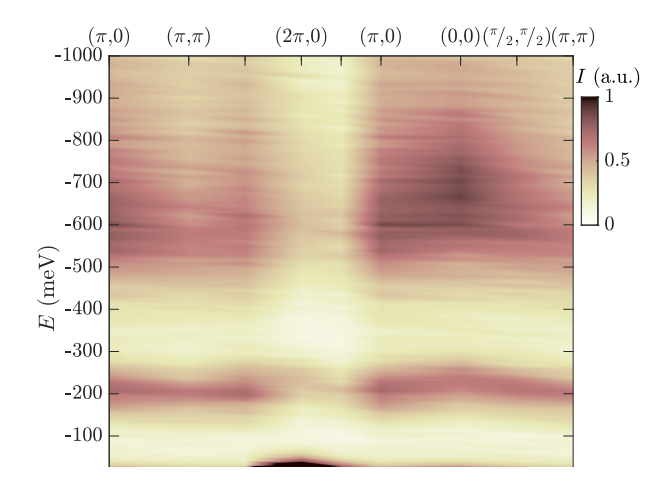
III. RESULTS

TABLE I. Low-energy Ir^{5+} $5d^4$ multiplet structure for $Sr_3Ir_2O_7F_2$ from *ab initio* calculations of a monomer $(IrO_6)^{7-}$ site and from RIXS experiments, approximated from Fig. 3. Values are in meV.

	MRCI+SOC		RIXS	
$3T_{1g}$	0	$(S_z = 0)$	0	elastic
	370, 440	$(S_z=\pm 1)$	170, 210	A, B
	580	$(\approx J=1)$	≈ 550	C
$^{1}T_{2g}, ^{1}E_{g}$	790, 820, 850		≈ 750	C
	960			intra- t_{2g}
	1700, 1730, 1780			intra- t_{2g}

We first discuss the results of the quantum chemistry simulations from the model of the isolated (IrO₆)⁷⁻ monomer (see Table I). Here the strong single-ion anisotropy and strong spin-orbit coupling are dominant. The S=1 ground state and first excited states are within the spin-orbit-split ${}^3T_{1g}$ manifold, so they are linear combinations of the d_{xy} , d_{xz} , and d_{yz} orbitals. The ab initio ground state has dominant in-plane orbital occupation. The first excited states are two spin-orbit-split levels akin to S_z=±1 near 300-400 meV. Another distinct ${}^3T_{1g}$ level is near 600 meV. At higher energies there are more intra- t_{2g} transitions to strongly spin-orbit-mixed ${}^1T_{2g}$, 1E_g configurations in the ranges 0.8-1.0 and 1.6-2.0 eV. These states' levels are likely an overestimation from neglecting partial occupation of the e_g manifold.

Now we compare these findings to the RIXS measurements in the quasi-2d Brillouin zone, shown as a map in Fig. 2(a). All measured excitations disperse weakly. We label the features (Table I and Fig. 3) as elastic at energy loss E=0, A at $E\approx170$ meV, B at $E\approx220$ meV, and C at $E\approx500$ -900 meV. A, B, and C are spin-orbit excitons. The A and B features match qualitatively with the ab initio model for the transitions from $S_z=0$ to $S_z=\pm1$. We note that no sharp features were observed in the optical



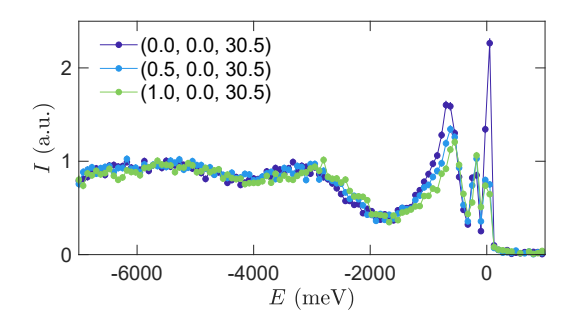


FIG. 2. (a) RIXS false-color map of raw intensities in the quasi-2d Brillouin zone. Ticks indicate the \mathbf{Q} positions where spectra were measured; the map was generated by interpolation. (b) Representative spectra for several \mathbf{Q} over a wide energy range to show higher-energy excitations. A constant background was subtracted from all scans in this figure.

conductivity from 0 to 1 eV, [6] consistent with feature C being composed of optically-forbidden spin-orbit excitons.

Higher energy features are visible in the spectra with a wider energy window shown in Figure 2(b). Near 1.3 eV there is a broad excitation in the optical conductivity, so the scattering may begin to include transitions across the charge gap. In the RIXS there is a broad peak at 3.2(1) eV, and at higher energies the scattered intensity is nearly flat. This is consistent with expectations for the $t_{2g}-e_g$ excitations, and establishes an approximate energy for the octahedral crystal field splitting. The high energy features also include contributions from O 2p-Ir t_{2g} charge-transfer scattering channels. [9, 10]

Next we comment on the widths of the low-energy RIXS features. For the A and B modes, the full width at half maximum (FWHM) values are very near 60 meV. This is near the 40 meV instrumental resolution and is much sharper than the other features, which precludes a collection of many modes. The bandwidth for the A and

B modes is about 15-35 meV, which points to weakly coupled excitations (i.e. high effective mass). The quantum chemistry model of the cluster $(Ir_2O_{11})^{12-}$ reveals that each of these modes is split by about 10 meV compared to the isolated $(IrO_6)^{7-}$ monomer, which supports our assertion that the dispersion is due to exchange coupling. The C feature has FWHM values near 100 meV, and a bandwidth of about 80 meV, consistent with a collection of many dispersive modes (confirmed from the many nearby modes in the quantum chemistry models). This broad feature is reminiscent of the broad spin-orbit excitons identified for Sr_2IrO_4 [11] and $Sr_3Ir_2O_7$ [12], systems where the tetragonal distortion is small and should weakly split the J=2 pentet for the J_{eff} =1/2 ground state.

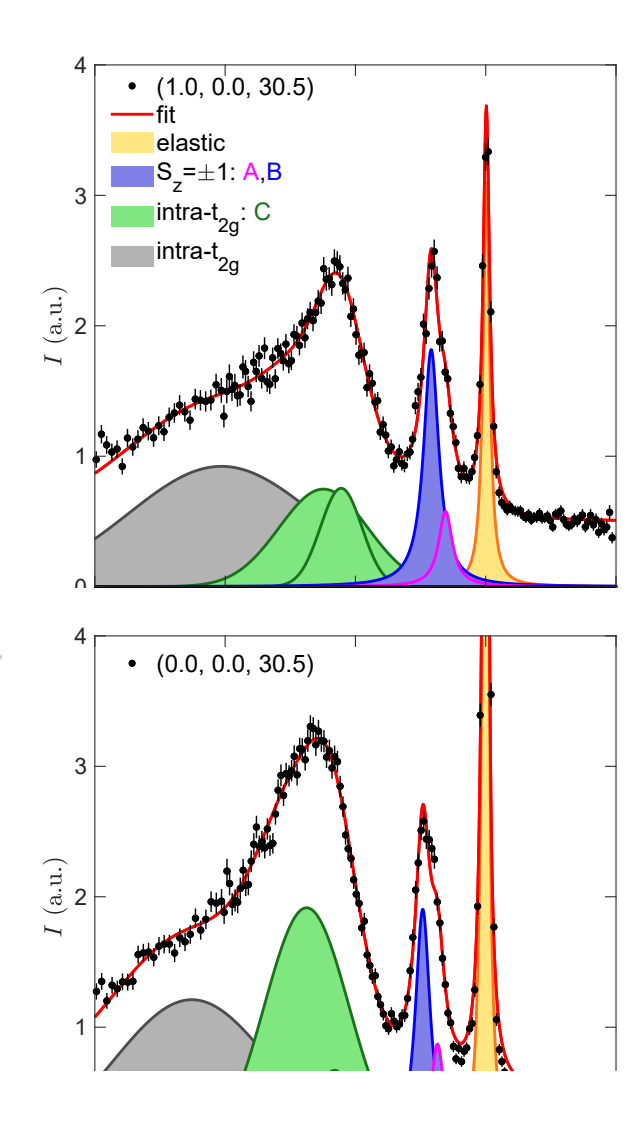
For the analysis of these RIXS features, the elastic line was fitted to a Voigt function, A and B were fitted to Lorenztians, and all other features were fitted to Gaussians. These peak shapes were chosen to empirically match the data. To attain well-behaved fits we found it appropriate to fix the A and B peaks' widths throughout this paper. The reduced chisquared χ^2_r (goodness-of-fit) values are nearly equal for fits where these parameters were fixed or free, as demonstrated in the Supplementary Information §S2. For the special case of tracking the l dependence of the A and B intensities at fixed h and k, the modes seem nondispersive so we fix the A and B peak energies as well, corroborated by the goodness-of-fit.

Using the fits as described above, we now consider the RIXS integrated intensities. Most features' intensities are nearly constant as functions of **Q**, with the exception of the A and B modes, which are nearly constant in the quasi-2d BZ yet exhibit a strong sinusoidal l dependence; see Fig. 4. The A mode intensity appears well-described by the functional form $sin^2(\pi ld/c)$, with d the bilayer Ir-Ir spacing and c the lattice constant. For the B mode the intensity variation is $\pi/2$ phase-shifted (to \cos^2) with an added constant background. We attribute this sinusoidal behavior of A and B to a double-slit-like interference for two different excited states that are delocalized across the bilayer. This interference effect results from the emission process in RIXS,[13] so it should be expected for RIXS spectra of all ions arranged like dimers, and it will not occur in the inelastic neutron scattering. A more detailed description of the physical origin and alternative explanations are provided in the discussion, subsection IVC.

IV. DISCUSSION

A. Model interpretation and electronic configuration

We begin our discussion with the spin-orbit exciton model, which we use to parameterize the experimental dispersion relation. First, we note that the model does not capture the sinusoidal variation in intensity along lbecause it is restricted to the (a,b) basal plane, so it



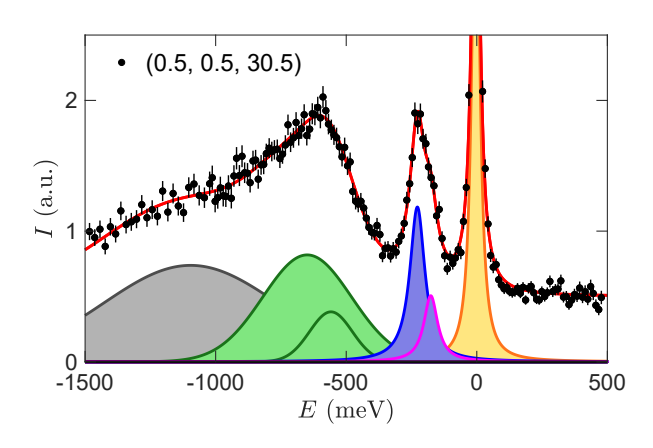
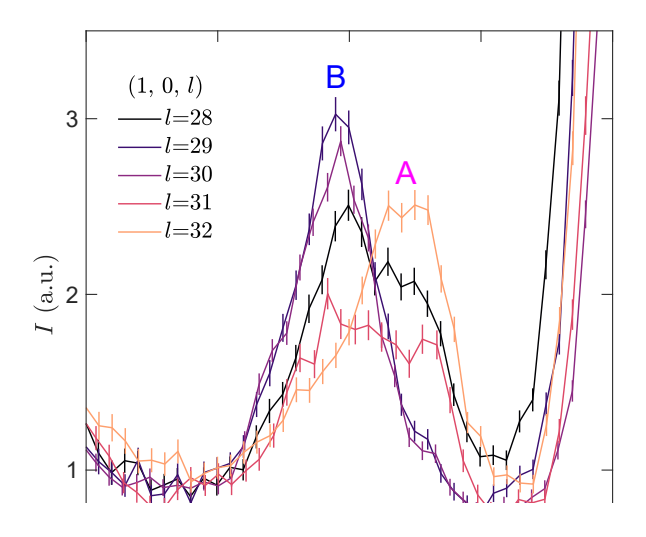


FIG. 3. Representative RIXS spectra (black dots) for several **Q**. Fits to the spectra (solid red lines) utilize the spectral components discussed in the text in addition to a constant background term.



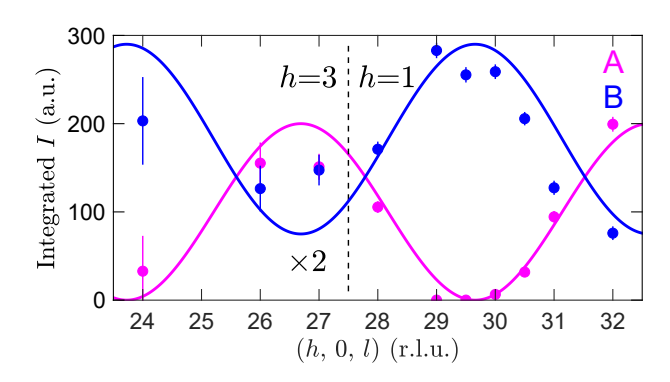


FIG. 4. (a) Raw RIXS spectra at (1,0,l) show the change in spectral weight of the A and B features (magenta and blue, respectively). (b) Integrated intensities of the Lorentzian fits to these features reveal sinusoidal dependence in l. The functional form of the magenta line is $sin^2(\pi ld/c)$, as is described in the text. Note that for $l{<}28$ the fitted scans were measured at (3,0,l) which was closer to normal incidence, where selfabsorption effects were larger due primarily to the scattering geometry. The $h{=}3$ scans were scaled by a factor of 2 to make the intensity values comparable.

only describes the quasi-2d BZ. The model assumes an idealized S=1 (L=1, J=0) regime.

By employing the refined parameters (Table II), the model produced two distinct modes with calculated dispersion relations in excellent agreement with the experimental data. As illustrated in Fig. 5, the A mode corresponds to transverse fluctuations ($\alpha\beta=+-$ and -+) within the basal plane of the pseudo-tetragonal unit cell, whereas the B mode at higher energy transfers corresponds to longitudinal zz fluctuations along the Ir⁵⁺ moment's axis. As summarized in Table II, the refined values for each of the five parameters exhibit close agreement (within 20%) with their initial values.

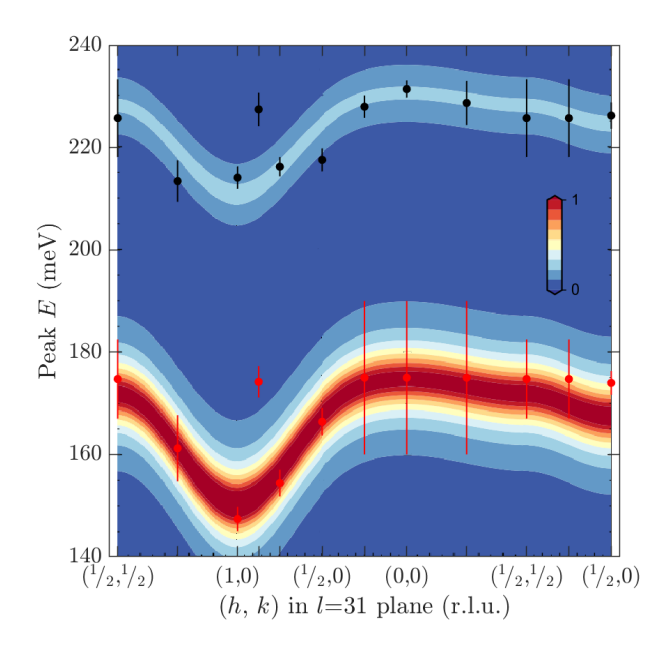


FIG. 5. Spin-orbit exciton model (solid colors and lines) in comparison to the fitted data (points). Energy transfers of transverse (lower energy) and longitudinal (higher energy) modes overplotted on $S(\mathbf{Q})$. Note that the RIXS intensity is not equivalent to $S(\mathbf{Q})$, and intensities have not been scaled to account for the scattering geometry. Error bars only account for peak energy uncertainty, and do not incorporate fixed widths $\approx 60 \text{ meV}$.

TABLE II. Refined parameter values of the spin-orbit exciton model for $\rm Sr_3 Ir_2 O_7 F_2$. All values are reported in meV and numbers in parentheses indicate calculated uncertainties.

Parameter	Initial Value	Range	Refined Value
$\alpha'\lambda$	200	[150,250]	187(5)
H_{MF}	0	[-5,5]	0.2(2)
δ	82	[40,120]	100(5)
J_1	2.1	[0,5]	2.1(1)
J_2	-1	[-2,2]	-0.80(5)

The refined value of 187(5) meV for the spin orbit coupling $\alpha'\lambda$ is comparable to values reported for other d^4 iridates [14]. The presence of one, rather than two, transverse modes can be understood by the negligible molecular field. According to the model, $H_{\rm MF}$ has a refined value of 0.2(2) meV, and this implies no splitting between the two plausible $\alpha\beta = +-$ and -+ transverse modes. The lack of a molecular field is also consistent with the absence of magnetic long-range order.

In such a case where the molecular field is absent, the gap between the longitudinal and transverse modes results from a uniaxial distortion of the coordination environment for a magnetic ion with unquenched orbital angular momentum. The large magnitude of δ with a refined value of 100(5) meV yields a significant gap of $\delta/2$. The positive sign fixes the longitudinal mode to higher energy transfers than the transverse mode. It can be shown [8] that the dispersion relation illustrated in Fig. 5 is indicative of an antiferromagnetic $J_1 > 0$ whose magnitude is greater than the ferromagnetic $J_2 < 0$.

To summarize, we interpreted the two lowest energy excitations as one transverse and one longitudinal S=1 exciton branch, split by a tetragonal distortion, with negligible molecular field. The modes disperse weakly according to weak couplings $J_{1,2}$. This interpretation is an oversimplified starting point, and we discuss the underlying assumptions further in the next sections.

B. Other considerations: electronic correlations and e_g mixing

We first comment on the electronic correlations. This paragraph is based entirely on the t_{2q} -only electronic configuration with S=1 and J=0 for comparison to our spin-orbit exciton model and other works. We estimate the Hund's coupling $J_H \approx 250$ meV based on work on the d^4 double perovskites.[14] We assume the ratio between Hund's coupling and the on-site Coulomb interaction is comparable to the precursor material Sr₃Ir₂O₇: $U\approx J_H/0.24=1 \text{ eV}$, [15] because this ratio is tied to charge carrier screening and both materials are insulators. Recent first-principles theoretical work supports this approximate value of U in the related d^5 compound Sr_2IrO_4 [16]. Therefore, we propose that $J_H \approx \alpha' \lambda$ in this rough estimate, which places this system in an intermediate regime between two limits: the low-SOC S=L=1 J=0 state and the high-SOC $J_{\rm eff}$ =0 singlet state described in the introduction. There is conjecture that the iridates are slightly closer to a jj coupling regime than the LS regime.[17]

If, instead of the above scenario, there is mixing in the $t_{2q}-e_q$ manifolds due to spin-orbit coupling as described by Stamokostas and Fiete, [18] then the electronic configuration would be quite different from what was considered elsewhere in this report. In this regime L=4 and S=1, yet $S_z=L_z=0$ so the total moment is still zero (J=0). We first note that this state and its sizeable e_q occupation of nearly 0.2 electrons is predicted based on the high value of $\langle L \cdot S \rangle = 3.5(3)$ computed from the Ir L-edge x-ray absorption branching ratio.[6] Such a high value is inconsistent with a t_{2q} -only J_{eff} model, which predicts $\langle L \cdot S \rangle \approx 2$. [18] Reconsidering the correlations in this context, we note that given the experimental uncertainty for the branching ratio and without an independent measurement of the spin quantum number, this model alone cannot be utilized to estimate the value of J_H .

C. Sinusoidal intensity dependence

Now we return to our consideration of the sinusoidal intensity dependence of the A and B modes along the l direction. When we consider possible explanations, we must satisfy the following observations:

- First, this effect must come from the Ir interactions along c such as across the bilayers, as it cannot be reconciled with isolated ab planes of Ir ions.
- Second, we note that these modes are large in magnitude and that the A intensity goes to zero within uncertainty at certain l values. Therefore, any explanation for the l dependence of the A and B features must be a significant effect that invokes the bulk d^4 state rather than defects.
- Third, given how dilute the RIXS-excited ions are in the measured sample, [19] we do not consider pairs of excitations on nearest-neighbor ions since these comprise weak scattering channels.

Based on these considerations for the sinusoidal l intensity dependence, we accredit the A and B features to spin-orbit excitons which form molecular orbitals that are delocalized across the bilayer. In x-ray emission measurements of ions arranged like dimers, such as RIXS performed on bilayers, the double-slit interference condition can be satisfied: the identity of which ion in the pair yielded the emitted photon, the 'slit' in this doubleslit experiment, cannot be determined in principle. An essential ingredient for the interference is delocalization of the photoexcited electron in the state intermediate to the absorption and the emission processes, which removes the 'which-path' information for the emitted photon. Related triplon (J=1) excitations are considered to be very delocalized for $5d^4$ materials. Similar delocalization is certainly occurring in-plane, yet the geometry of the Ir-O planes does not allow for double-slit interference.

Furthermore, the delocalization of the exciton leads to the most natural microscopic picture for the observed A and B features: symmetric and antisymmetric molecular orbital excited states that form across the bilayer. The most consistent picture is one of the two crystal field split $S_z{=}\pm 1$ states hybridizing with the $S_z{=}0$ ground state; howver we note that this is not explicitly captured in the ab initio simulations. To explain the phase shift between these two features that yields the sin^2 and cos^2 dependence along l, we turn to the RIXS scattering amplitude derivation in the Appendix. The argument is adapted from Refs. 20–22. For visualization purposes the symmetric and antisymmetric orbitals can improperly be considered as akin to bonding and anti-bonding states.

This interference phenomenon was measured in detail for structural dimer systems including $Ba_3CeIr_2O_9$, with Ir_2O_9 bioctahedra that have small Ir-Ir separations $d=2.5\text{\AA}$ along the c axis.[20, 23] The dimerized Ir sites'

molecular orbitals are delocalized, giving rise to interference among several distinct excited states in RIXS measurements. As a result, the intensity of transitions to the excited states for Ba₃CeIr₂O₉ modulates sinusoidally along l, where symmetric intermediate states vary as $\sin^2(\pi ld/c)$ and antisymmetric intermediate states vary as $\cos^2(\pi ld/c)$.[20] In contrast to Sr₃Ir₂O₇F₂, this dimer example has much closer Ir ions with a different valence and wildly different electronic configurations. Crucially the dimer system has a much larger orbital overlap parameterized by the hopping $t\approx 1$ eV along c. However, we propose that the excitons in the present study are delocalized, with the Ir-O-Ir bonding providing enough orbital overlap to result in modest hopping for the exciton.

Instead of the proposed electronic configuration, one could envision magnetic or orbital dimerization as a means of interpreting the sinusoidal intensity dependence. For instance, if there are many O vacancies then there could be interlayer-dimerized Ir⁴⁺ defects, since these may not have a strong signature in the bulk susceptibility. However, this magnetic dimerization seems unrealistic based on how dilute unpaired Ir⁴⁺ ions are <1 mol percent and also the structural refinements. On the other hand, we cannot rule out Ir⁵⁺ orbital ordering and dimerization based on the existing evidence. In the $3d^2$ compound $Sr_3Cr_2O_7$, the proposed ground state is an interlayer orbital singlet state which yields a qualitatively similar crystal field environment. [24] Orbital ordering or dimerization could plausibly explain why the bilayer Ir spacing d does not decrease with holes from $Sr_3Ir_2O_7$ to Sr₃Ir₂O₇F₂, even though the Ir free ionic radius decreases 9% from the 4+ to the 5+ valence.

Yet another explanation for the sinusoidal intensity variation is acoustic and optical transverse paramagnon modes, which could possibly exist along with a longitudinal mode. Acoustic(optical) modes are known to have a $sin^2(cos^2)$ dependence on the wavevector along the bilayer direction l.[25] In this explanation, the oberved splitting 50 meV translates to intra-bilayer coupling $J_c \approx 25 \text{ meV.} [26]$ This sizeable interlayer coupling (much greater than $J_{1,2}$) would imply dimer excitations that are weakly coupled in-plane. However, the primary inconsistency with this interpretation lies in the roomtemperature coupling J_c which is at odds with the established paramagnetic ground state for 2 K < T < 400K. Also, it is difficult to imagine such strong anisotropy for the paramagnons, since in-plane and out-of-plane Ir-Ir distances are comparable.

D. Extension of the results

We now revisit the interpretation of the RIXS measurements of the canted antiferromagnet bilayer system $Sr_3Ir_2O_7$. There, the geometry and delocalization required for double-slit interference in the emission process are present for spin orbit excitons — in this case, exci-

tations of holes from the $J_{\text{eff}}=1/2$ ground state to the $J_{\text{eff}}=3/2$ quartet [11]. In the RIXS study of $Sr_3Ir_2O_7$ performed by Moretti Sala and co-workers there are two low-energy features in the range of 80 to 180 meV, split by about 30-70 meV, that are attributed to longitudinal and transverse magnon modes.[27] The interpretation of acoustic and optical modes is ruled out based partially on the in-plane dependence of the intensity. In summarizing the results we note that: (a) the intensity and energy dependence of the two features track well in-plane; and (b) when l is changed the two features modulate strongly in intensity but not in energy (see also Ref. 15). These observations do not rule out the longitudinal/transverse interpretation. However, we propose that, to some extent, these effects may be attributable to a double-slit-like interference among spin-orbit excitons across the bilayer. Future measurements, with more spectra at different l, can help determine which of these interpretations is valid.

We now extend the spin-orbit exciton model for other d^4 systems. In considering materials such as $\mathrm{Ca_2RuO_4}$ with strong tetragonal distortions, the S_z states seem valid, especially considering that $e_g - t_{2g}$ mixing is much less important at the lower spin-orbit coupling in 4d compounds.

As for $(Sr,Ba)_2YIrO_6$, the...

V. SUMMARY

In conclusion, we measured resonant inelastic x-ray scattering for the $5d^4$ band insulator $\mathrm{Sr_3Ir_2O_7F_2}$ and interpret the low-energy excitations with quantum chemistry simulations as well as a spin-orbit exciton model. We comment on the electronic configuration of the system and the relevant energy scales including effective spin-orbit coupling, tetragonal distortion, exchange coupling, and correlations, in the context of related systems based on Ir, Ru, and Os sites. The strong interference effect along the bilayer direction is a consequence of x-ray emission. We echo previous predictions that interference effects can be significant in dimer, bilayer, and related systems studied via RIXS.

Appendix: Derivation of the RIXS interference

This derivation is a slightly modified reproduction of the supplemental materials to Ref. 20. In the dipole and fast-collision approximations, [21, 22] the Ir L_3 RIXS

scattering amplitude $A_f(q)$ of one final state $|f\rangle$ is:

$$A_f(q) \propto \langle f | \sum_{\mathbf{R}} e^{i\mathbf{Q}\cdot\mathbf{R}} [D^{\dagger}(\epsilon_{out})D(\epsilon_{inc})]_R | i \rangle$$
 (A.1)

where $|i\rangle$ denotes the initial (ground) state, ϵ the polarization of incident and outgoing photons, D the local dipole transition operator, and R runs over all Ir sites that contribute to the final state $|f\rangle$. If we consider a final state that accounts for two Ir sites across the bilayer at $\mathbf{r}_{1,2}=(0,0,\pm d/2)$ then, since they are equivalent sites, the matrix elements may only differ in sign. If we measure the dependence along l at $|\mathbf{Q}|=2\pi l/c$ we get:

$$A_f(q) \propto e^{i\mathbf{Q}\cdot\mathbf{r}_1} \pm e^{i\mathbf{Q}\cdot\mathbf{r}_2} \propto \begin{cases} sin(\pi ld/c) \\ cos(\pi ld/c) \end{cases}$$
 (A.2)

The intensity (scattering cross section) is $I(q,\omega) = \sum_f |A_f(q)|^2 \delta(\hbar\omega - E_f)$ where $\hbar\omega$ is the outgoing photon energy and E_f is the excited state energy. Therefore, symmetric and antisymmetric levels yield sin^2 and cos^2 dependences along l, as observed for the A and B features respectively.

ACKNOWLEDGMENTS

The authors acknowledge useful discussions with A. Revelli, C. Stock, H. Lane, B.R. Ortiz, K.J. Camacho, and C. Schwenk. This work was supported by NSF award DMR-1729489 (S.D.W. and Z.P.). P.M.S. acknowledges additional financial support from the University of California, Santa Barbara, through the Elings Fellowship. The research made use of the shared facilities of the NSF Materials Research Science and Engineering Center at UC Santa Barbara, Grant No. DMR-1720256. We also acknowledge the use of the Nanostructures Cleanroom Facility within the California NanoSystems Institute, supported by the University of California, Santa Barbara and the University of California, Office of the President. Use of the Advanced Photon Source at Argonne National Laboratory was supported by the U. S. Department of Energy, Office of Science, Office of Basic Energy Sciences, under Contract No. DE-AC02-06CH11357. This material is based upon work supported by the National Science Foundation's Q-AMASE-i initiative under award DMR-1906325.

^[1] G. Khaliullin, Phys. Rev. Lett 111, 197201 (2013).

^[2] O. N. Meetei, W. S. Cole, M. Randeria, and N. Trivedi, Phys. Rev. B 91, 054412 (2015).

^[3] The effective spin-orbit coupling of d^4 ions is reduced by a factor of 2 from d^5 ions; see Ref. 28.

^[4] A. Paramekanti, D. J. Singh, B. Yuan, D. Casa, A. Said, Y. J. Kim, and A. D. Christianson, Phys. Rev. B 97, 235119 (2018).

^[5] S. Mohapatra, J. Van Den Brink, and A. Singh, Phys. Rev. B 95, 094435 (2017).

- [6] C. Peterson, M. W. Swift, Z. Porter, R. J. Clément, G. Wu, G. H. Ahn, S. J. Moon, B. C. Chakoumakos, J. P. C. Ruff, H. Cao, C. Van De Walle, and S. D. Wilson, Phys. Rev. B 98, 155128 (2018).
- [7] A. Jain, M. Krautloher, J. Porras, G. H. Ryu, D. P. Chen, D. L. Abernathy, J. T. Park, A. Ivanov, J. Chaloupka, G. Khaliullin, B. Keimer, and B. J. Kim, Nat. Phys. 13, 633 (2017).
- [8] P. M. Sarte, C. Stock, B. R. Ortiz, K. H. Hong, and S. D. Wilson, Phys. Rev. B 102, 245119 (2020).
- [9] K. Ishii, I. Jarrige, M. Yoshida, K. Ikeuchi, J. Mizuki, K. Ohashi, T. Takayama, J. Matsuno, and H. Takagi, Phys. Rev. B 83, 115121 (2011).
- [10] V. M. Katukuri, H. Stoll, J. Van Den Brink, and L. Hozoi, Phys. Rev. B 85, 220402 (2012).
- [11] J. Kim, D. Casa, M. H. Upton, T. Gog, Y. J. Kim, J. F. Mitchell, M. Van Veenendaal, M. Daghofer, J. Van Den Brink, G. Khaliullin, and B. J. Kim, Phys. Rev. Lett 108, 177003 (2012).
- [12] J. Kim, M. Daghofer, A. H. Said, T. Gog, J. Van Den Brink, G. Khaliullin, and B. J. Kim, Nat. Commun. 5, 4453 (2014).
- [13] Y. Ma and M. Blume, Rev. Sci. Instrum 66, 1543 (1995).
- [14] B. Yuan, J. P. Clancy, A. M. Cook, C. M. Thompson, J. Greedan, G. Cao, B. C. Jeon, T. W. Noh, M. H. Upton, D. Casa, T. Gog, A. Paramekanti, and Y. J. Kim, Phys. Rev. B 95, 235114 (2017).
- [15] J. Kim, A. H. Said, D. Casa, M. H. Upton, T. Gog, M. Daghofer, G. Jackeli, J. Van Den Brink, G. Khaliullin, and B. J. Kim, Phys. Rev. Lett. 109, 157402 (2012).
- [16] C. Lane, Y. Zhang, J. W. Furness, R. S. Markiewicz, B. Barbiellini, J. Sun, and A. Bansil, Phys. Rev. B 101, 155110 (2020).
- [17] H. Gretarsson, H. Suzuki, H. Kim, K. Ueda, M. Krautloher, B. J. Kim, H. Yavaş, G. Khaliullin, and B. Keimer, Phys. Rev. B 100, 045123 (2019).
- [18] G. L. Stamokostas and G. A. Fiete, Phys. Rev. B 97, 085150 (2018).

- [19] Here, flux $\sim 10^{12}/s$ and the excited volume contains $\sim 10^{15}$ Ir ions. These values imply that pairs of excitations caused by the incident photons are infrequent for realistic final excited state lifetimes < s.
- [20] A. Revelli, M. Moretti Sala, G. Monaco, P. Becker, L. Bohatý, M. Hermanns, T. C. Koethe, T. Fröhlich, P. Warzanowski, T. Lorenz, S. V. Streltsov, P. H. van Loosdrecht, D. I. Khomskii, J. van den Brink, and M. Grüninger, Sci. Adv. 5, eaav4020 (2019).
- [21] L. J. Ament, G. Khaliullin, and J. Van Den Brink, Phys. Rev. B 84, 020403 (2011).
- [22] B. J. Kim and G. Khaliullin, Phys. Rev. B 96, 085108 (2017).
- [23] Y. Wang, R. Wang, J. Kim, M. H. Upton, D. Casa, T. Gog, G. Cao, G. Kotliar, M. P. Dean, and X. Liu, Phys. Rev. Lett. 122, 106401 (2019).
- [24] J. Jeanneau, P. Toulemonde, G. Remenyi, A. Sulpice, C. Colin, V. Nassif, E. Suard, E. Salas Colera, G. R. Castro, F. Gay, C. Urdaniz, R. Weht, C. Fevrier, A. Ralko, C. Lacroix, A. A. Aligia, and M. Núñez-Regueiro, Phys. Rev. Lett. 118, 207207 (2017).
- [25] D. Reznik, P. Bourges, H. F. Fong, L. P. Regnault, J. Bossy, C. Vettier, D. L. Milius, I. A. Aksay, and B. Keimer, Phys. Rev. B 53, R14741 (1996).
- [26] T. G. Perring, D. T. Adroja, G. Chaboussant, G. Aeppli, T. Kimura, and Y. Tokura, Phys. Rev. Lett. 87, 217201 (2001).
- [27] M. Moretti Sala, V. Schnells, S. Boseggia, L. Simonelli, A. Al-Zein, J. G. Vale, L. Paolasini, E. C. Hunter, R. S. Perry, D. Prabhakaran, A. T. Boothroyd, M. Krisch, G. Monaco, H. M. Ronnow, D. F. McMorrow, and F. Mila, Phys. Rev. B 92, 024405 (2015).
- [28] A. Abragam and B. Bleaney, Electron paramagnetic resonance of transition ions (Oxford University Press, 2012).